Available online at www.sciencedirect.com
SCIENCE DIRECT®
Polymer 45 (2004) 2711–2719
polymer
www.elsevier.com/locate/polymer

Morphological transitions of spinodal decomposition in confined geometry

Xiaorong Wang[a,*], Naruhiko Mashita[b]

[a]Bridgestone/Firestone Research Center, 1200 Firestone Parkway, Akron, OH 44317-001, USA
[b]Chemical and Industrial Products Materials Development Department, Bridgestone Corporation, 1 Kashio-cho, Totsuka-ku, Yokohama, Kanagawa 244-8510, Japan

Received 10 October 2003; received in revised form 10 December 2003; accepted 12 December 2003

Abstract

We studied the phase separation of a polymer solution in thin slabs of thickness of micrometers. The material used was an asymmetrical binary system that consisted of 6 wt% semi-crystalline poly(ethylene butene) (or cEB) and 94 wt% of diisodecyl adipate (or DIDA) solvent. The de-mixing mechanism in the confined geometry is very different from that in bulk. Phase separation in bulk usually starts with formation of the solvent holes, and polymer-rich phase becomes a micro-reticulated network. While, in thin films the phase separation starts with formation of the polymer-rich droplets, that behave like Brownian particles. We have observed that there exists a critical thickness L_c below which the size of the droplets decreases drastically. Above the critical thickness, we have observed a phase morphological transformation from droplets to chains, branches, and then to networks, which follows a very similar pattern of a percolation process. There is correspondingly a second critical thickness L_c^* ($> L_c$) below which no bi-continuous phase separation takes place.

Keywords: Phase separation; Confinement; Morphological transition

1. Introduction

Spinodal decomposition (SD) in polymer solutions produces fascinating network structures or patterns [1–14]. The reason is that the polymer-rich phase (or the dynamically slow component) during phase separation becomes more and more visco-elastic with time. The initial growth of the concentration fluctuations in those systems is soon suppressed by the formation of the slow-component phase [1–8]. The resultant process is then governed by a competition between thermodynamics and visco-elastics. The formation of the final morphological structure is usually a consequence of a unique combination of thermodynamics and visco-elastics. Of importance is that the pattern evolutions observed in a polymer solution are essentially the same to that in a polymer blend of different T_gs [14]. Understanding the phenomenon and the process is pertinent because they are of intrinsic importance not only in industrial materials developments [1,9,10] but also in fundamental investigations [15–17]. There has been considerable theoretical and experimental work on describing the characteristic features of those systems [17–22]. The main results are summarized in a recent review by Tanaka [23].

Some years ago, researchers in our group developed a new technology, namely the frozen-in SD, to create polymeric foams and gels of skeleton-like reticulated networks of cell sizes of few micrometers [1–4,9,10]. In that study, a small amount of a semi-crystalline polymer (~10 wt%) was first mixed with a low molecular weight solvent at an elevated temperature to obtain a homogeneous solution. Then, the homogeneous binary mixture was allowed to cool or quench into the unstable part of its miscibility gap. As a result, a spontaneous growth of the long wavelength concentration fluctuations (i.e. SD) took place in the system, and a bi-continuous phase morphology was formed. The phase pattern was then preserved or frozen by the crystallization of the polymer in the polymer-rich phase upon further cooling. The key principle in the technology is the fine-tuning of the solvent quality for that the crystallization of the polymer occurs just below the miscibility gap.

* Corresponding author.

0032-3861/$ - see front matter © 2004 Elsevier Ltd. All rights reserved.
doi:10.1016/j.polymer.2003.12.076

The resultant material is a micro-reticulated network that can have a very dense distribution of uniform cells. Varying the cooling rates, solvent quality, and the compositions can control the cell sizes. After removing the low molecular weight solvent from the polymeric reticulate structure, there is also obtained a three-dimensional continuous network skeleton that is consisting essentially of the pure polymer. This network is capable of effectively trapping a variety of other low molecular weight materials and has found a wide variety of applications [9,10], such as in liquid crystal displays, battery cell separators, membrane filters, and high damping additives. In addition to the technological importance, the frozen-in technology also provides the opportunity in fundamental studies of SD processes. Especially, the technology can freeze any moment of the evolution in the phase separation for detail investigations. In this paper, we intend to discuss the phase separation of a polymer solution in slab geometry of thickness of micrometers. As to be shown, the de-mixing structures in a thin slab are quite different from that observed in bulk.

2. Experimental section

Semi-crystalline poly(ethylene-*co*-butene) (or cEB) with a molecular weight of $M_n = 2.2 \times 10^4$ and $M_w/M_n = 1.28$ was from JSR under commercial name: Dynaron E6100P. The blocked copolymer was made from hydrogenation of an anionically polymerized low vinyl–high vinyl–low vinyl block polybutadiene. The melting index of the polymer was 0.6 g/10 min at 230 °C/2.16 kg (based on the ASTM D1238). The melting point T_m of the polymer was 98 °C. The crystallinity of the polymer was about 40%. The gravity density ρ of the polymer at 23 °C was 0.88 g/cm^3. The polymer was used without further purification.

Diisodecyl adipate (or DIDA), 99% purity, was from the C.P. Hall Company. The material was a clear colorless liquid, and had a viscosity of about 30 cps and a density of 0.918 g/cm^3 at 23 °C. Prior to the use, the DIDA solvent was filtered through a micro-membrane of about 0.2 μm pore size. This precaution is important for minimizing dust effects on phase separation.

The cEB polymer was first swelled and then dissolved into the DIDA solvent at approximately 150 °C. Complete dissolution took place within 1 h with vigorous stirring. Once it became clear, the solution was then diluted to 6 wt% concentration. The solution was homogeneous and transparent at temperature $T > 110$ °C. The phase separation temperature of the solution was 105 °C. The crystallization temperature of the polymer in the DIDA solution was about 90 °C. Fig. 1 shows the phase diagram of the cEB/DIDA system. The open circles in the plot represent the cloud points. The selected concentration, i.e. 6 wt%, is near the critical point of the phase diagram and thus guarantees a SD-induced phase separation when quenched. The concentration dependence for the crystallization temperature is very weak and has been omitted from the phase diagram.

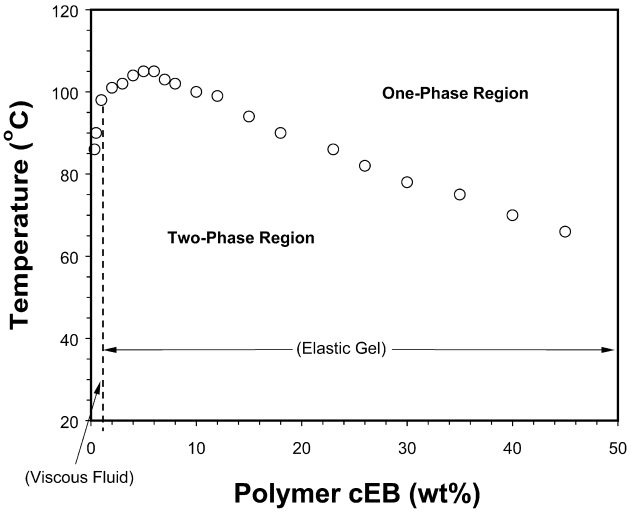

Fig. 1. Phase diagram for semi-crystalline poly(ethane butene) (or cEB) and diisodecyl adipate (or DIDA).

To make a wedge-like thin film, a small drop of the hot solution was first placed on a pre-cleaned 25 mm wide × 75 mm long × 1 mm thick microscope glass slide. On the top of the liquid drop was then covered with a microscope cover glass of 22 wide × 26 mm long × 0.17 mm thick. Between the two glasses, a strip-like spacer of thickness of about 10 μm was used on the one side of the microscope slides. The liquid that was sandwiched between the two slides was then pressed to form a wedge-like liquid film. The thickness of the film changed gradually from 0 to 10 μm over a length of 25 mm. The preparation was carried on a hot stage of temperature higher than 120 °C. Two kinds of glass surfaces, including the hexamethyldisilazane-treated and untreated surfaces, were used in the film preparation to compare the surface wetting effects on the phase separation.

To make a planar thin film, a small drop of the hot solution was first placed on a pre-cleaned 10 mm diameter × 0.2 mm thick microscope glass that was glued on a spin-coater SCX-50 (from Novocontrol GmbH). Then, the planar thin film was made by letting the small drop to spin at a speed ranging from 1000 to 6000 rpm. A heat gun was used to keep the surface temperature of the glass higher than 120 °C. An IR laser thermometer (from Extech) was used to monitor the surface temperature. Variation in film thickness was achieved by varying the temperature and the spin speed.

Phase separation in those films was monitored using a Carl Zeiss optical microscope equipped with a Mettler FP52 hot stage that was controlled by a Mettler FP90 control processor. Usually a sample film was first equilibrated at 150 °C for 20 min. Then, the sample film was either cooled down to 23 °C at a cooling rate 10 °C/min or quenched to 100 °C and then hold there isothermally, depending on the experiment needs. Phase evolution in the film was imaged

using an instant Polaroid camera that had been loaded with plate-like sheet films.

3. Results and discussion

The cEB/DIDA solution is homogeneous and transparent at temperature $T > 110\ ^{\circ}C$. It can turn into opaque once it is brought to a temperature $T \leq 100\ ^{\circ}C$. Initially, usual growth of concentration fluctuations occurs throughout the system when it is cooled. Modulated structure due to the SD is observed. Then, the solvent-rich phase starts to appear as holes and the holes grow with time. After that, the phase separation manner is changed from a fluid-like mode to a gel-like mode. With the growth of solvent holes, the polymer-rich phase becomes network structure [1]. Finally, when temperature reaches the crystallization point of the polymer, the phase structure is frozen, and the resultant material is bi-continuous micro-reticulated network. Fig. 2 shows a typical phase structure of the system in bulk, after being cooled from 150 to 23 °C at a cooling rate of 10 °C/min. The resultant structure is a polymer-rich skeletal network and a solvent-rich continuous phase. The structure is quite stable at room temperature and the material is typically elastic.

The pattern evolution observed in bulk is similar to that reported by Tanaka [6–9,11] for a dynamically asymmetric system that composes of a fast component (or solvent) and a slow component (or polymer). Phase separation in such a case strongly depends on the visco-elastic characteristics of the two components. Because of its long relaxation time, the polymer-rich phase can catch up with the deformation rate of the phase separation. Thus, the phase separation often leads to the formation of a long-lived network of the slow component (or the polymer) though its concentration <10 wt%. An important difference in our system is the existence of the crystallization during the phase separation.

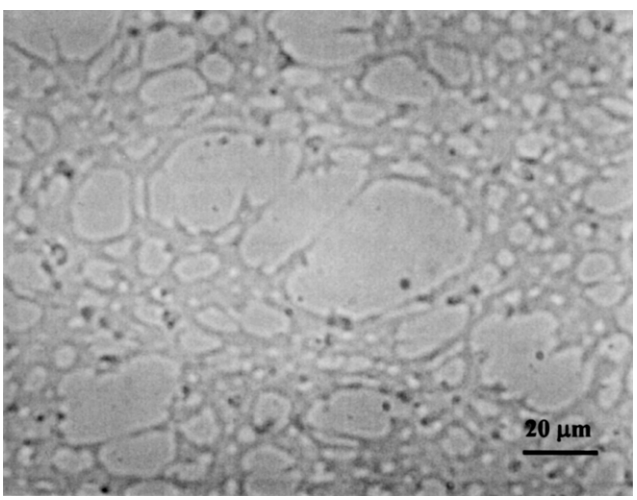

Fig. 2. Phase structure of a 6 wt% cEB/DIDA solution in bulk, after cooled from 150 to 23 °C at a cooling rate of 10 °C/min.

The crystallization of the polymer provides the opportunity to freeze any moment in the phase evolution upon cooling.

The formation of the network-like or sponge-like structure of the polymer-rich phase is generally transient in nature, though the transient state may last for hours in common experimental time-scale. Without the crystallization, the super-network structure will eventually collapse in late stages of the phase separation, as driven by the free energy minimization of the system. Hence, the phase separation structure obtained (see Fig. 2) by fast cooling represents only an early period of the phase separation. Typically, it represents a phase evolution of 2–3 min of the polymer solution after a strict temperature quench from 120 to 90 °C. Because it is of practical significance [9,10], our interest in this research is concentrated on this early-time episode.

When the polymer solution is confined into a thin slab, however, the phase separation structures are quite different from that observed in the bulk conditions. Fig. 3 shows the microscope observations on a wedge-like film of the polymer solution. The thickness of the film varies from 0 to 10 μm over the wedge length of about 25 mm. After being cooled down from 150 to 23 °C at a cooling rate of 10 °C/min, the film is examined under a microscope and pictures are taken from various positions. When the thickness of the film is smaller than $L_c \cong 0.8$ μm (see Fig. 3(a)), phase separation cannot be observed under the optical microscope. Above this critical thickness L_c, the film shows some phase separation, but the initial morphology appears to be very small polymer-rich droplets (see Fig. 3(b)). As the thickness increases, the droplets increases in size and the morphology then gradually change to chains (see Fig. 3(c)), and then the chains are gradually transformed to branches (see Fig. 3(d) and (e)). The size of branches gradually grows (see Fig. 3(f)–(h)) as the thickness reaches to a critical value, i.e. $L_c^* \cong 3.7$ μm. Above the second critical thickness L_c^*, the branches are linked together (see Fig. 3(i)–(k)). For films of thickness $L > 6$ μm the phase structure returns back to the reticulated network (see Fig. 3(l)) that looks like the morphology in bulk (see Fig. 2). The thickness L has a dominating effect on the phase separation. A schematic drawing of the phase morphology with increase of the film thickness is shown in Fig. 4.

The area fraction of polymer-rich domains, Φ_{area}, can be obtained by a black-and-white operation on the photo pictures (see Fig. 3) using an imagine analyzer. The thickness L dependence of Φ_{area} for a wedge-like film is plotted in Fig. 5. As L approaches L_c ($\cong 0.8\ \mu m$) from below, the fraction of polymer-rich domains Φ_{area} shows a rapid jump around the critical point. Above L_c, the quantity Φ_{area} levels and stays almost constant for a wide range of thickness. The film in this range shows phase separation, but the initial morphology appears to be droplets. For $L > L_c$, the droplet size is almost constant. However, for $L < L_c$, the droplet size decreases drastically with decreasing the film thickness (see the insert in

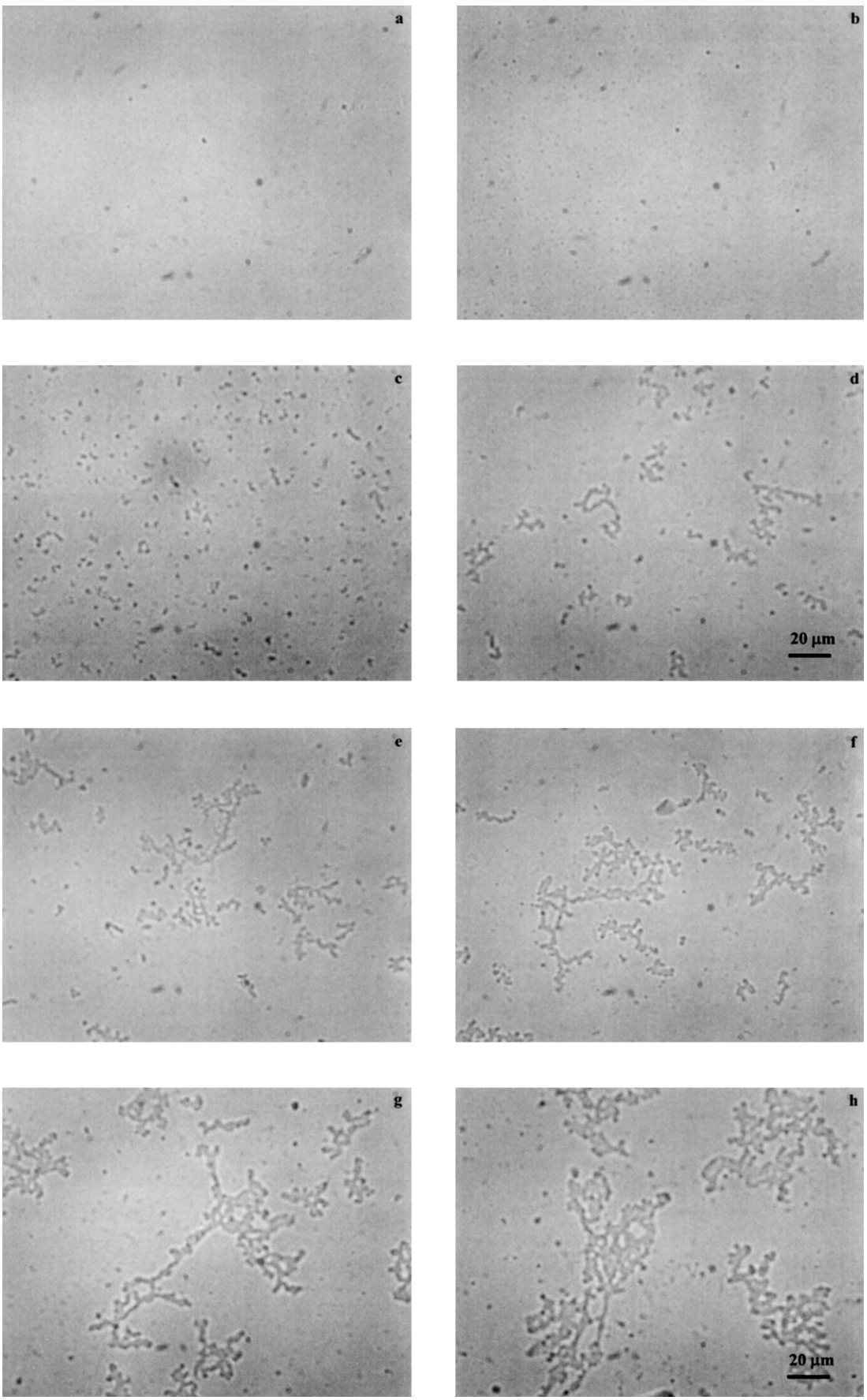
a
b
c
d
20 μm
e
f
g
h
20 μm

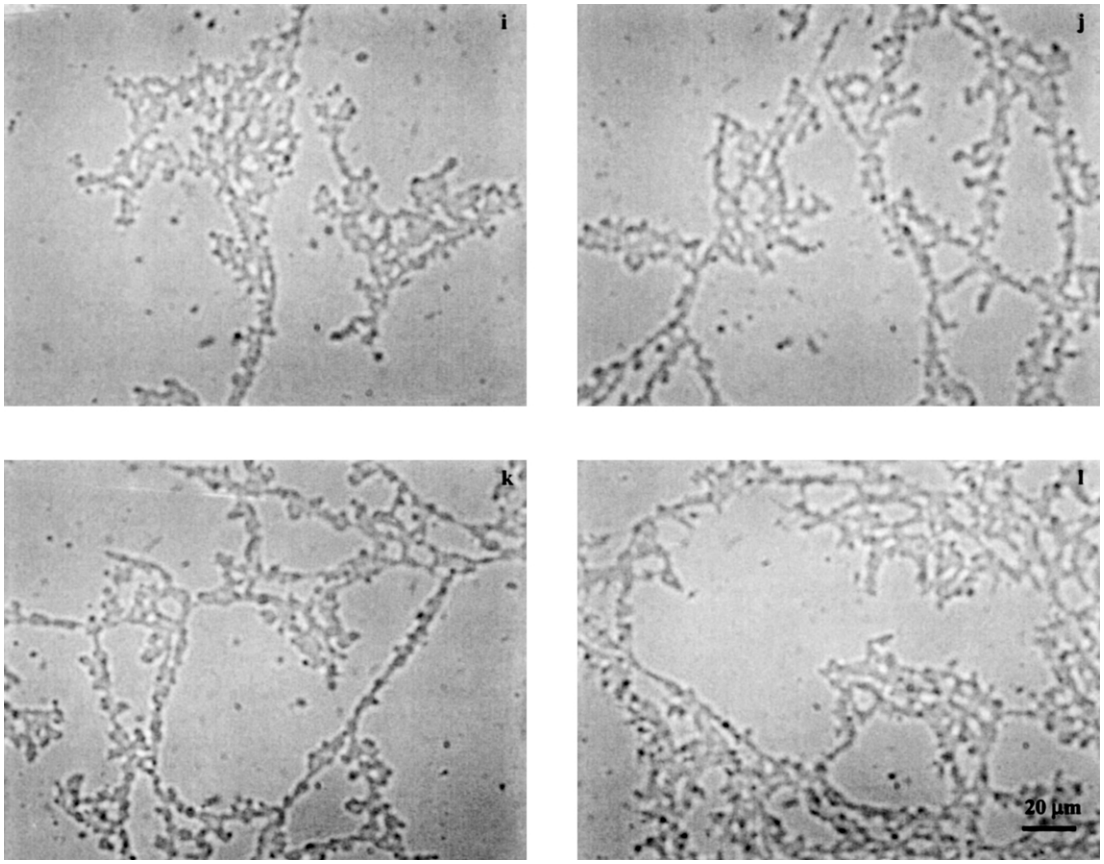

Fig. 3. Phase structures of a 6 wt% cEB/DIDA solution in a wedge-like film geometry, after cooled from 150 to 23 °C at a cooling rate of 10 °C/min. Pictures are taken at various positions. ((a) $L = 0.8$ μm, (b) 1.2 μm, (c) 1.6 μm, (d) 2.0 μm, (e) 2.4 μm, (f) 2.7 μm, (g) 3.5 μm, (h) 4.3 μm, (i) 4.8 μm, (j) 5.1 μm, (k) 5.5 μm, (l) 6.3 μm).

Fig. 5). This transition suggests that below L_c the thin film constraint on the phase separation is much stronger than that above L_c, for it primarily acts on reducing the size of droplets. The rapid change in Φ_{area} when $L < L_c$ is probably due to the optical resolution of a microscope. The optical resolution usually cuts off the phase separation that occurs on scales much smaller than the wavelength of visible light.

Further increasing the thickness L, we see a phase morphological transformation from droplets to chains, branches, and then to networks. Here, we employ the scheme of average spatial radii $\langle \xi_n \rangle$ and $\langle \xi_w \rangle$ to analyze the size evolution in polymer-rich phase during the transformation; where $\langle \xi_n \rangle = \Sigma n_i \xi_i / \Sigma n_i$ and $\langle \xi_w \rangle = \Sigma n_i^2 \xi_i / \Sigma n_i \xi_i$. The size ξ_i is the spatial radius of a given polymer-rich object (e.g. a droplet, chain, or branch) and n_i is the number of the object. Fig. 6 shows the average spatial radii $\langle \xi_n \rangle$ and $\langle \xi_w \rangle$ as a function of the film thickness L. Interestingly, $\langle \xi_w \rangle$ increases much quicker than $\langle \xi_n \rangle$, and shows a tendency to diverge when system approaches the second critical thickness $L_c^* \cong 3.7$ μm. This divergence of $\langle \xi_w \rangle$ suggests that the thickness dependence of the morphological structure in a confined space follows a very similar pattern of a percolation (or gelation) process [24,25]. From a physical view of point, percolation (or gelation) may be conceived as the point beyond which a network structure is formed. Fig. 7 shows a linear plot of the number average of the polymer-rich domain fraction $\Phi_{area}/\Sigma n_i$ vs. the film thickness L. The linear relationship in the plot indicates that $\Phi_{area}/\Sigma n_i$ in the phase separation is analogue to the average reacted mass M_n in a chemical gelation, and the film thickness L in the phase separation is analogue to the chemical conversion in the gelation process [24].

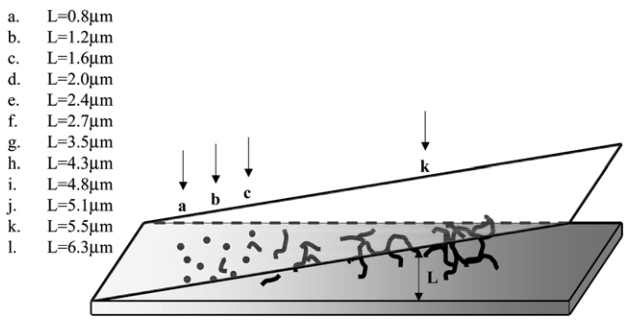

Fig. 4. A schematic drawing of the morphology change observed in a wedge-like film geometry.

The existence of critical thickness in phase separation process is surprising, especially under confinement of micrometer sizes. Our first speculation of the reason could be due to the special geometry of the wedge-like film. We

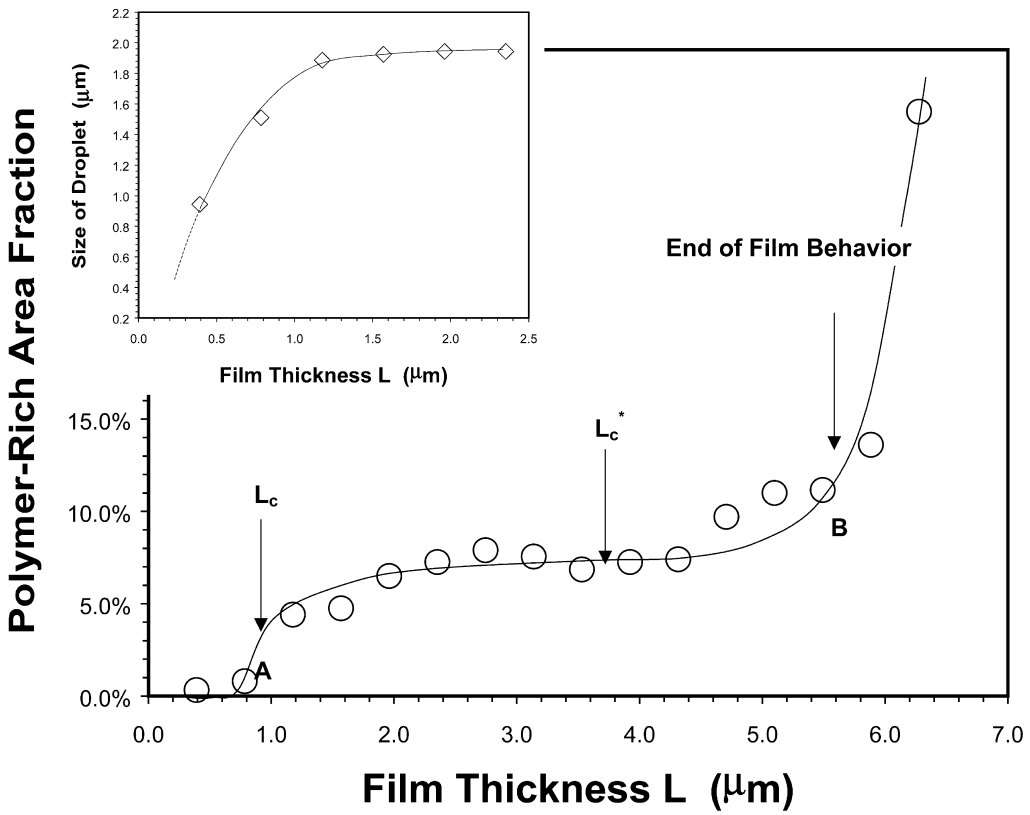

Fig. 5. A plot of the area fraction of polymer-rich domains Φ_{area} vs. the film thickness L. The insert is a plot of the droplet size vs. the film thickness L.

therefore prepared a number of planar films in which one surface was in contact with a microscope glass slide but the other surface was exposed to air. Nevertheless, the same phase separation structures in wedge-like films are observed in the planar films. Again, for films of thickness $L > L_c^*$, the polymer-rich phase is a reticulated network structure after cooling. While, for films of thickness $L < L_c^*$, only droplets and branched chain structures present in the mixture (see Fig. 8). In addition, we also prepared planar films on hexamethyldisilazane-treated glass slides. The surface hydroxyl groups of the slides have been converted to trimethysilyl groups, which should provide better wetting for organic solutions. However, the same morphological transformation was observed. Accordingly, the de-mixing behavior for the binary system in confined slabs, as discussed above, cannot be interpreted in terms of the influences from a wedge-like geometry or from the glass surfaces, though the influence of surface wetting on the phase separation process has become an important issue in material science [26–31].

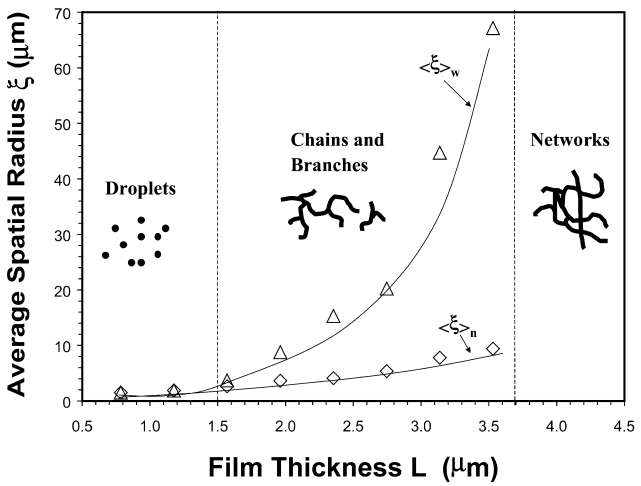

Fig. 6. A plot of the average spatial radii, $\langle \xi_n \rangle$ and $\langle \xi_w \rangle$, vs. the film thickness L.

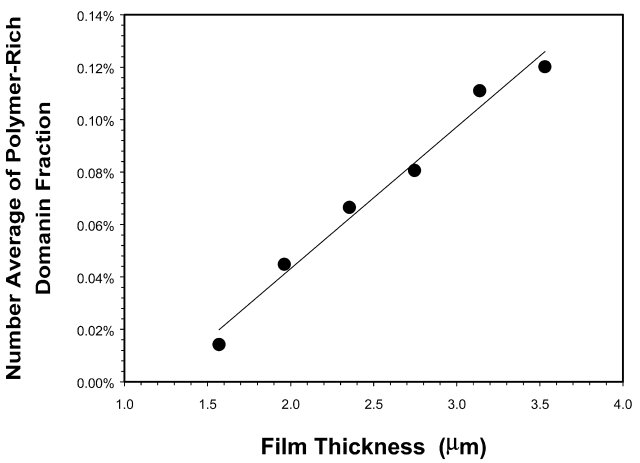

Fig. 7. A plot of the number average of the polymer-rich area fraction $\Phi_{area}/\Sigma n_i$ vs. the film thickness L.

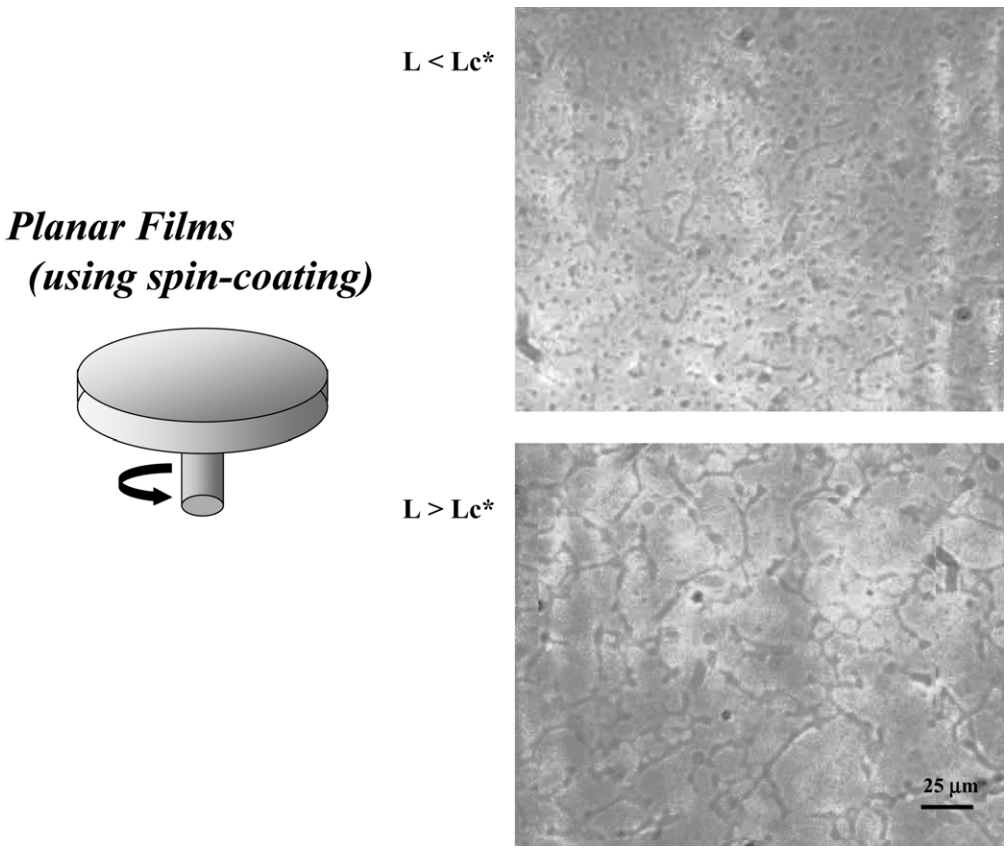

Fig. 8. Phase structures of a 6 wt% cEB/DIDA solution in planar thin film geometry, after cooled from 150 to 23 °C at a cooling rate of 10 °C/min.

Our second speculation of the reason for the anomalous phase transformation could be due to the transient nature of phase structures. The droplet morphology might be the early state of the network morphology, and the crystallization of the polymer might have frozen the phase evolutions into different states. To answer this question, we have investigated the phase evolution on planner films at 100 °C isothermally, which is 5 K below the phase separation temperature 105 °C, but 10 K above the crystallization temperature 90 °C of the polymer in the solution. For films of thickness $L \gg L_c^*$ (i.e. $L > 10$ μm), just after a temperature quench, the sample first becomes cloudy and then microscopic solvent holes come into view. The number and the size of the holes increase with time, and some of them then start to coalesce. The polymer-rich phase accordingly becomes network-like structure. The formation of the network usually takes less than 30 s, but the network can persist for hours at 100 °C. As time increases, the network eventually breaks into pieces, which then round up and collapse into big islands. However, for films of thickness $L_c < L \ll L_c^*$ (i.e. $L \cong 1 \sim 2$ μm), phase separation starts with the formation of polymer-rich phase droplets after the temperature quench. The droplets once created are almost uniform in size and are moving freely by Brownian motion. Some of the droplets then stick together to form chains and branches, but frequently they break-up again. An important fact is that this droplet morphology is very stable (see Fig. 9) and can last for a day at 100 °C. After that, slowly some of the droplets coalesce together and form big islands. The droplet morphology in fact is more stable than the network morphology. It is therefore unlikely that the droplet morphology is the early state of the network morphology or vice versa. It is also highly improbable that the discovered morphological transition rises from the different stages of the phase separation. Our observation suggests that phase separation in bulk and thick films starts with formation of solvent holes. While, in thin films the phase separation starts with formation of droplets of polymer molecules.

Finally, does the polymer concentration play an important role in the anomalous phase morphologies observed in thin films? To answer this question, we have investigated a number of solutions of various polymer concentrations ranging from 4.5 to 12 wt%. Nevertheless, the same morphological transformation is observed in all those solutions as long as they are confined in the thin film geometry. The only difference is that, as polymer concentration increases, the solution viscosity increases and the time for phase separation increases. Our experiments also extend further on the phase separations of non-crystalline poly(ethylene-*co*-propylene) rubbers (or EPRs) in the diisodecyl adipate (or DIDA) solvent. Again, the phase separation for those non-crystalline systems shows the same morphological transformation in the thin film geometry.

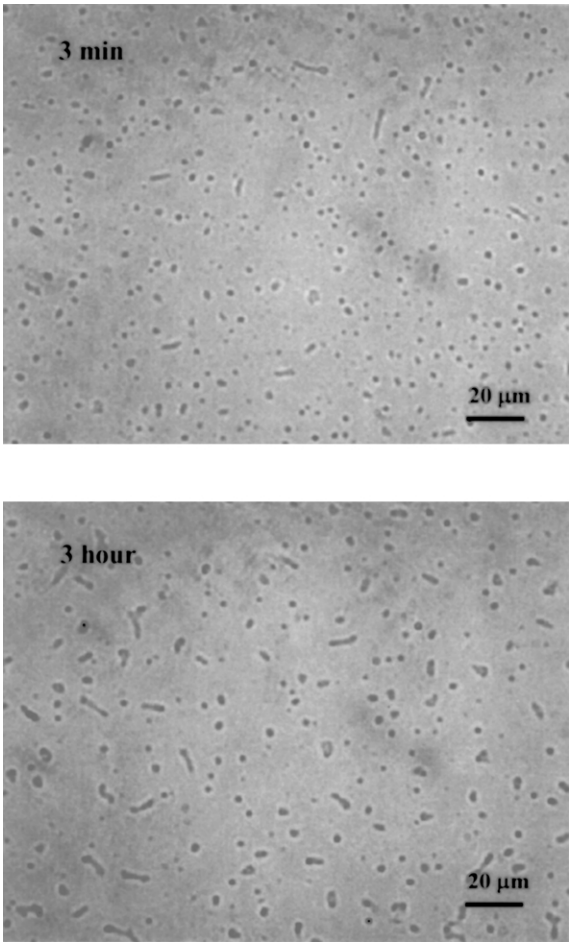

Fig. 9. Phase evolution of droplet morphology of a 6 wt% cEB/DIDA solution in planar thin film (~1.5 μm thickness) at 100 °C isothermally, after quenched from 150 to 100 °C.

Under those circumstances, it would be reasonable to assume that the dynamically asymmetrical differences between the polymer and the solvent in the solution may have been suppressed when the two components are confined in a thin film geometry, since the phase separation observed in a thin film geometry is indeed very similar to common dynamically symmetrical systems observed elsewhere [12–20]. As expected, in the thin film geometry (e.g. when $L = 1-2$ μm) the polymer-rich phase of micro-scales once formed will be under a pressure. The pressure tensor P due to the confinement should act additionally to the osmotic stress Π due to the concentration fluctuations. Accordingly, the thermodynamic driving forces will act asymmetrically on polymer-rich phase and solvent-rich phase during the phase separation. The growth rate of polymer-rich phase may apparently speed up and become comparable to that of solvent molecules as the film thickness decreases. As a result, the polymer solution in thin film geometry behaves as dynamically symmetric systems and forms polymer-rich droplets in the early stage of the phase separation. However, in bulk and thick films (i.e. when $L > 10$ μm), because the growth rate of solvent-rich phase is usually much faster than that of the polymer-rich phase, the solvent molecules form holes first despite it is the majority component. As the holes grow with time, the polymer-rich phase becomes a network skeleton. Somewhere between the two extremes, there will be expected a percolation-like morphological transformation as the one being observed. This tentative explanation, nevertheless, needs independent experimental and theoretical studies.

4. Conclusion

For the cEb/DIDA solutions confined in film geometry, the SD-induced phase separation of a polymer solution displays two characteristic events with increasing the film thickness. In thin films of thickness of 1–2 μm, the phase separation starts with the formation of polymer-rich droplets. In thick films of thickness >10 μm, the phase separation starts with the formation of the solvent holes, and the polymer-rich phase become a micro-reticulated network. Between the two extremes, the phase structure displays a morphological transformation from droplets, to chains, branches, and then to networks, which follows a very similar pattern of a percolation process. For films thickness <1 μm, there is a drastically decrease in the size of the droplets with decreasing the thickness. Although the mechanism has not been clarified yet, our experimental results do suggest that those transitions are not caused by the different stages of the phase separation or rises from the behavior of surface wetting.

References

[1] Fukahori Y, Mashita N. Polym Adv Technol 2000;11:472.
[2] Mashita N, Fukahori Y. Polym J 2000;34(10):719.
[3] Fukahori Y, Mashita N. Polym Prepr Jpn 1995;44:1738.
[4] Mashita N, Fukahori Y. Kobunshi Ronbunshu 2000;57(9):596.
[5] Tanaka H, Nishi T. Jpn J Appl Phys 1988;27:L1787.
[6] Tanaka H. Macromolecules 1992;25:6377.
[7] Tanaka H, Miura T. Phys Rev Lett 1993;71:2244.
[8] Tanaka H. J Chem Phys 1994;100:5323.
[9] USP5451454, USP5716997, EP0699710A2, USP5910530, USP6048930.
[10] JP3310108, JP3336648, JP3298107, JP3376715, JP3378392.
[11] Tanaka H. Phys Rev Lett 1996;76:787.
[12] Hashimoto T, Itakura M, Hasegawa H. J Chem Phys 1986;85:6118.
[13] Bates FS, Wilzius P. J Chem Phys 1989;91:3258.
[14] Binder K. Adv Polym Sci 1991;112:181.
[15] de Gennes PG. J Chem Phys 1980;72:4756.
[16] Pincus P. J Chem Phys 1981;75:1996.
[17] Onuki A. J Chem Phys 1986;85:1122.
[18] Kawasaki K. Macromolecules 1989;22:3063.
[19] Kotnis MA, Muthukumar M. Macromolecules 1992;25:1716.
[20] Larson RG. The structure and rheology of complex fluids. Oxford: Oxford Univesity Press; 1999.
[21] Haas CK, Torkelson JM. Phys Rev Lett 1995;75:3134.
[22] Tanaka H. Phys Rev E 1997;56:787.
[23] Tanaka H. J Phys: Condens Matter 2000;12:R207–64.

[24] Flory PJ. Principles of polymer chemistry. Ithaca, NY: Conell University Press; 1953.
[25] de Gennes PG. Scaling concepts in polymer physics. Ithaca, NY: Conell University Press; 1977.
[26] Fischer HP, Maass P, Dieterich W. Eurphys Lett 1998;42(1):49.
[27] Ball RC, Essery RLH. J Phys: Condens Matter 1990;2:13303.
[28] Jones RAL, Norton LJ, Kramer EJ, Bates FS, Wiltzius P. Phys Rev Lett 1991;66:1326.
[29] Bruder F, Brenn R. Phys Rev Lett 1992;69:624.
[30] Fischer HP, Maass P, Dieterich W. Phys Rev Lett 1997;79:893.
[31] Jinnai H, Kitagishi H, Hamano K, Nishikawa Y, Takahash M. Phys Rev E 2003;67:21801.